

# Tribological properties of electrospark deposited coatings by a CoCrFeNiW electrode

Xiaoming Chen<sup>1</sup>, Xiaodong Chai<sup>1\*</sup>, Liang Chang<sup>2</sup>, Zijun Wang<sup>1</sup>, Guanglin Zhu<sup>1</sup>, Cean Guo<sup>1</sup>, Jian Zhang<sup>1</sup>

<sup>1</sup>*School of Equipment Engineering, Shenyang Ligong University, Shenyang 110159, P. R. China*

<sup>2</sup>*Troops 96853 of the People's Liberation Army, Shenyang 110084, P. R. China*

Received 15 July 2024, received in revised form 11 March 2025, accepted 13 March 2025

## Abstract

A coating on a CrNi3MoVA steel substrate was prepared by electrospark deposition technology with an equiatomic sintered electrode of a high-entropy CoCrFeNiW alloy. SEM, EDS, and XRD were used to investigate the morphology, composition and phase structure of the CoCrFeNiW high-entropy alloy coating. The tribological behavior of coating under different loads was investigated using a reciprocal friction and wear tester. The results showed that the as-deposited CoCrFeNiW coating with a hardness of 9.78 GPa is composed of face-centered cubic (FCC) and Cr<sub>2</sub>O<sub>3</sub>; compared with the CrNi3MoVA steel, the CoCrFeNiW coating has an obvious antifriction effect at 6 and 9 N load; the CoCrFeNiW coating remarkably increases the wear resistance of the CrNi3MoVA steel.

**Key words:** high-entropy alloy, CoCrFeNiW coating, electrospark deposition, tribological properties

## 1. Introduction

The key components of some equipment have been used in conditions of high-speed friction for a long time, and their service time directly affects the life of the whole equipment. These key components have high manufacturing costs and complex manufacturing process characteristics. Extending their life under the working conditions of high-speed friction and wear is an urgent problem to be solved in materials science.

Since Yeh et al. [1] and Cantor et al. [2] proposed the concept of high-entropy alloy (HEA) in their respective research work in 2004, HEAs have attracted extensive attention from researchers all over the world for their excellent properties, such as hardness, wear resistance and high-temperature oxidation resistance, etc., and they have become a research focus for their promising application prospect. The preparation techniques of the bulk HEAs are complex, so they cannot be widely used in industry. The manufacturing process of some key components is especially complicated, resulting in a long manufacturing replacement cycle, which is extremely unfavorable for emergency

service needs. HEA coatings can avoid the complex manufacturing process and inherit the excellent properties of HEAs. Therefore, they can be widely used in aerospace, military, machinery and other fields.

In the current research, the CoCrFeNi-based HEA coatings are attractive, especially the properties of AlCoCrFeNi coatings. AlCoCrFeNi is one of the earliest manufactured HEAs, and extensive research has been done on the performance of its coatings. However, compared with the AlCoCrFeNi coatings, there is much less research on CoCrFeNiW coatings, and the element W can improve the hardness and wear resistance of HEA in contrast to the element Al. Liu H. et al. [3] used laser cladding technology to prepare HEA coatings of CoCrFeNiW<sub>x</sub> ( $x = 0, 0.25, 0.5, 0.75, 1.0$ ), and the results showed that the CoCrFeNiW coating exhibits good wear resistance at an elevated temperature of 600 °C due to the formation of the oxide layer on the worn surface.

Among the preparation technologies of HEA coatings, electrospark deposition (ESD) technology has many advantages, such as low equipment cost, easy operation, strong coating bonding strength, etc. [4–6].

\*Corresponding author: e-mail address: [tcd87@163.com](mailto:tcd87@163.com)

Table 1. Chemical composition of CrNi3MoVA steel (wt.%) [7]

Cr	Ni	Mo	V	Mn	C	Si	P	S	Fe
1.28	3.14	0.37	0.20	0.41	0.40	0.25	0.012	0.001	Balance

Table 2. Specific process parameters of CoCrFeNiW coating

Voltage (V)	Power (W)	Capacity ( $\mu\text{F}$ )	Duration (s)	Energy of pulse (J)	Electrode rotating rate ( $\text{r min}^{-1}$ )	Ar gas flow ( $\text{L min}^{-1}$ )	Deposition time unit area ( $\text{min cm}^{-1}$ )
60	1200	420	$10^{-6}$ – $10^{-5}$	0.756	2000	12	2

Especially for the local repair of key components with special shape features, the coating prepared by ESD has a more uniform thickness and good accessibility. To the authors' knowledge, there is still little relevant research on the tribological properties of CoCrFeNiW coatings deposited on a steel substrate by ESD technology. In this work, a CoCrFeNiW coating was prepared on a CrNi3MoVA steel by ESD technology, and its microstructure, mechanical properties and tribological properties were investigated. This investigation aims to fabricate a CoCrFeNiW coating with excellent wear resistance on a steel substrate using ESD technology and elucidate the coating's forming process and wear resistance.

## 2. Materials and methods

### 2.1. Preparation of CoCrFeNiW coatings

CrNi3MoVA steel was selected as the substrate material because it is commonly used as a key component material of equipment under the service condition of severe wear, and its chemical composition is shown in Table 1 [7]. The CrNi3MoVA steel bar was cut into cuboid samples with a 20 mm  $\times$  10 mm  $\times$  4 mm dimension by the SYJ-400 automatic precision cutting machine. The samples were polished with SiC sandpapers with a roughness (Arithmetical Mean Deviation of the Profile,  $Ra$ ) from 12.5  $\mu\text{m}$  to 0.05  $\mu\text{m}$  and then polished with diamond paste with a size of 2.5  $\mu\text{m}$  to obtain a roughness ( $Ra$ ) of 0.02–0.04  $\mu\text{m}$ . After that, the samples were placed into a container of anhydrous alcohol and cleaned by ultrasonic wave for 300 seconds. Then, they were immediately dried with a hair dryer.

The electrode material is made of Co, Cr, Fe, Ni, and W powders with a purity of more than 99.9%, and the average size of the powder diameter is approximately 400 nm. The CoCrFeNiW alloy was prepared using the spark plasma sintering (SPS) technique by mixing the powders in a predetermined proportion (equal atomic ratio). The CoCrFeNiW alloy

was wire cut into a cylindrical electrode with a size of  $\phi$  5 mm  $\times$  50 mm and polished to remove the oxide layer from the surface by using SiC sandpaper to obtain a roughness ( $Ra$ ) of 4  $\mu\text{m}$ , and then also cleaned by ultrasonic wave in anhydrous ethanol for 10 min, and immediately blown dry.

A DJ-2000 metal surface repair machine was employed as ESD equipment, and the CoCrFeNiW alloy electrode was clamped by a fixture in the deposition gun and exposed a length of 20 mm, and the coating was prepared on the CrNi3MoVA steel under argon protection. The specific optimum process parameters after the preliminary experiment are shown in Table 2.

### 2.2. Characterization and property testing of CoCrFeNiW coatings

The surface morphologies and elemental composition of the CoCrFeNiW coatings were characterized by scanning electron microscope (SEM, TESCAN VEGA3, Czech Republic) equipped with an energy dispersive X-ray spectrometer (EDS, X-MAX, UK), respectively. The phase structure of the coating was obtained by X-ray diffraction (XRD, X'Pert PRO, Holland). The hardness and elasticity modulus of the CrNi3MoVA and CoCrFeNiW coatings were tested by using nanoindentation G200 with a Berkovich indenter and calculated by the Oliver-Pharr model through loading curves, and the values are the mean values of the tested eight points. The friction and wear tests of the CrNi3MoVA and CoCrFeNiW coatings with different loads (3, 6, and 9 N) were carried out at room temperature by employing an HSR-2M reciprocating friction and wear tester. The load value can be obtained from the pressure sensor, which is the load to apply vertically on the sample's surface. A 304 stainless steel ball with a diameter of 6 mm was selected as one of the friction pairs, and other parameters of the friction and wear test are shown in Table 3. The number of parallel friction tests is five times, and the friction coefficient values were the average of all five tests.

Table 3. Parameters of friction and wear test

Reciprocation distance (mm)	Temperature (°C)	Running time (min)	Reciprocation times ( $t \text{ min}^{-1}$ )
5	23	20	500

Table 4. EDS results of three regions of CoCrFeNiW coating

Element (at.%)	Co	Cr	Fe	Ni	W
C	17.40	14.44	32.60	19.46	16.10
D	6.10	48.69	32.77	8.40	4.05
E	17.26	13.12	34.04	19.58	15.96

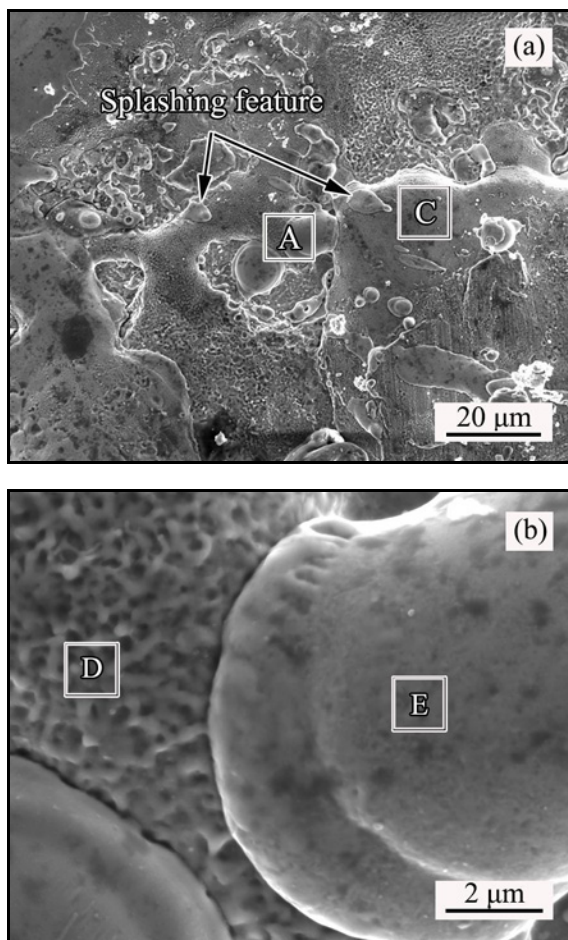


Fig. 1. Surface morphologies of as-deposited CoCrFeNiW coating at low (a) and high (b) magnifications.

### 3. Results

#### 3.1. Microstructure and phase structure

Figure 1 shows the surface morphologies of the as-deposited CoCrFeNiW coating at different magnifications. As shown in Fig. 1a, a typical splashing fea-

ture on ESD coatings [8–11] (marked with arrows) appears on the as-deposited CoCrFeNiW coating, resulting from the rapid solidification of the melting metal, which causes the coating surface to be uneven. Abdi et al. [9] proposed that splashing is the most effective factor in heat loss of coating efficiency at high spark energy. The roughness ( $Ra$ ) of the as-deposited coating is  $0.77 \mu\text{m}$ , measured by a confocal laser scanning microscope (CLSM, LS4000, Japan). Region A between two globes is magnified in Fig. 1b. It can be observed that there are some micro-globes in Fig. 1b, and the globular-shaped islands are also a typical feature of the ESD technique [10]. The globe's surface is compact, even though the surface in between has some micro-holes of CoCrFeNiW coating. Table 4 shows the EDS results of the three regions (C in Fig. 1a, D and E in Fig. 1b) of the CoCrFeNiW coating. As shown in Table 4, regions C and E have almost the same content of Co, Cr, Fe, Ni, and W, which is far different from the content of the as-sintered electrode, for the content of Fe is much higher than that of the other four elements. It needs to be noted that the Cr content is the lowest among the other four elements. However, the content of Cr is the highest among the five elements in region D.

Figure 2 shows the cross-sectional morphology of the as-deposited CoCrFeNiW coating and its EDS line scanning results. As shown in Fig. 2a, the thickness of the coating is about  $38.4 \mu\text{m}$ , and it is free of cracks and has a compact microstructure. The EDS line scanning results from the top of the coating to the substrate (Fig. 2b) show that the elements of Co, Cr, Ni, W, and Fe have a gradient transition between the coating and the substrate, indicating a strong metallurgical bond between the CoCrFeNiW coating and the CrNi3MoVA steel substrate, which has a beneficial effect to enhance the coating performance. Although the strong metallurgical bond between substrate and coating has been reported by many investigations due to the interinfiltration of the electrode and the substrate [12–14], the bond should be much stronger for the Fe element is in both the electrode and the sub-

Table 5. Nanoindentation results of CrNi3MoVA steel and CoCrFeNiW coating

Samples	$H$ (GPa)	$E$ (GPa)	$H/E$	$H^3/E^2$
CrNi3MoVA	4.68	262.8	0.0178	0.0015
CoCrFeNiW coating	9.78	232.3	0.042	0.017

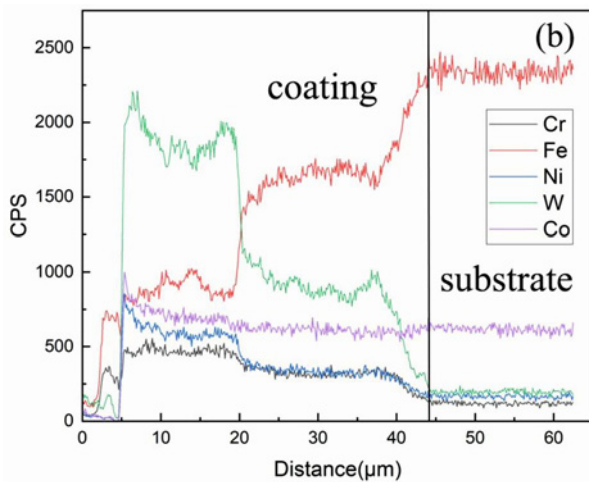
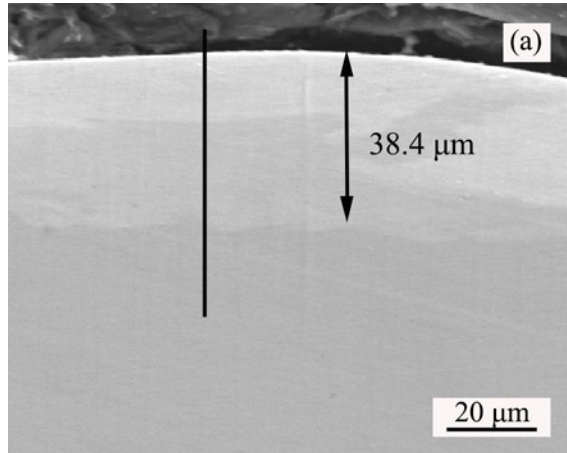


Fig. 2. Cross-sectional morphology of as-deposited CoCrFeNiW coating (a) and its EDS line scanning results (b).

strate, which has been verified by the EDS line scanning results (Fig. 2b).

Figure 3 shows the XRD pattern of the as-deposited CoCrFeNiW coating. As shown in Fig. 3, the as-deposited CoCrFeNiW coating is composed of face-centered cubic (FCC) and  $\text{Cr}_2\text{O}_3$ , which suggests that oxidation occurred during the ESD CoCrFeNiW coating process. Combining with the EDS results of region D (Fig. 1b and Table 4), it can be inferred that the  $\text{Cr}_2\text{O}_3$  morphology is between two globes (Fig. 1b). Therefore, the EDS results agree with the XRD pattern of the CoCrFeNiW coating. Different from the FCC, unmelted W and  $\text{Fe}_7\text{W}_6$  phases in

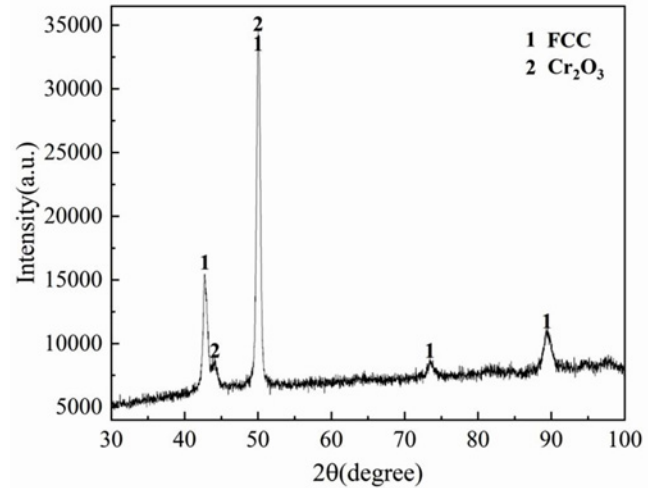


Fig. 3. XRD pattern of as-deposited CoCrFeNiW coating.

the CoCrFeNiW coating prepared via laser cladding on AISI1045 steel [3], the CoCrFeNiW coating fabricated by ESD has only one FCC phase except for the oxide phase, indicating that the ESD process can be beneficial to the formation of a homogeneous coating. Xie Y. J. et al. [15] obtained a homogeneous coating composed of only the single  $\gamma$  phase by ESD technique when they used the less homogeneous NiCoCrAlYTa electrode with a dual phase  $\gamma/\beta$  structure, which shows the same advantage as our experimental results.

### 3.2. Nanoindentation results of CrNi3MoVA steel and CoCrFeNiW HEA coating

Table 5 shows the nanoindentation results of the CrNi3MoVA steel and the CoCrFeNiW coating. As shown in Table 5, compared with the CrNi3MoVA steel, the hardness ( $H$ ) of the CoCrFeNiW coating increases about 1.1 times and the elasticity modulus ( $E$ ) reduces by 11.6%, which favors the increase of  $H/E$  and  $H^3/E^2$  of the CoCrFeNiW coating, two of the main parameters relative to friction and wear performance of materials, and they will be discussed later.

### 3.3. Friction coefficients and worn mechanism of CrNi3MoVA steel and CoCrFeNiW coating

Figure 4 shows the friction coefficients of the CrNi3MoVA steel and the CoCrFeNiW coating at 3,

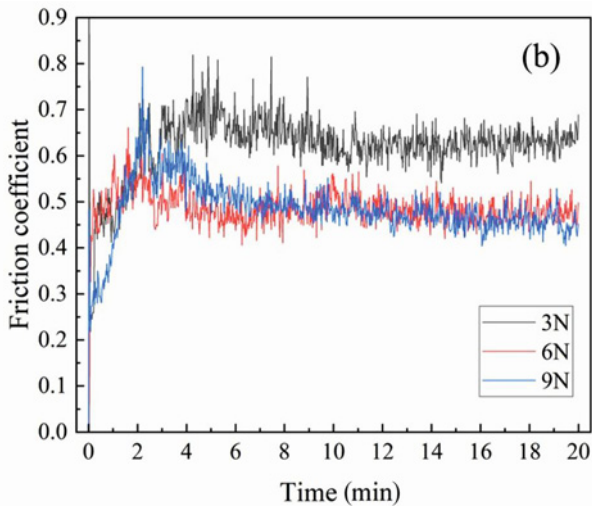
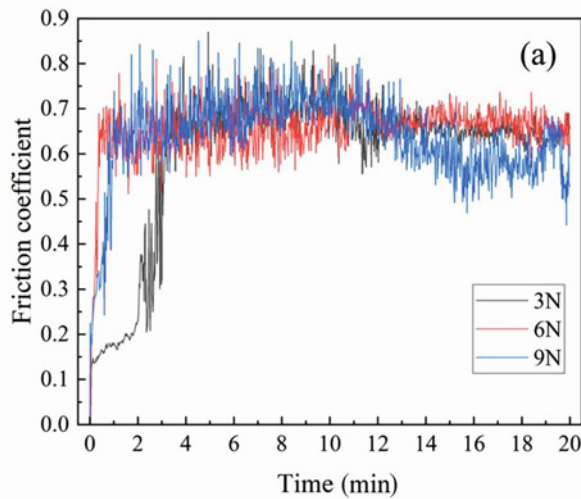


Fig. 4. Friction coefficients of CrNi3MoVA steel (a) and CoCrFeNiW coating at 3, 6, and 9 N load (b).

6, and 9 N load. As shown in Fig. 4a, in the first ten minutes, the change of the load almost has no influence on the coefficients of the CrNi3MoVA steel, and after that, all three friction coefficients begin to reduce, and the friction coefficient at 9 N load has the biggest reduction. As shown in Fig. 4b, the friction coefficients at 6 and 9 N load are almost the same in the steady state, much smaller than the friction coefficient at 3 N load. Compared with the CrNi3MoVA steel, the CoCrFeNiW coating has an obvious anti-friction effect at 6 and 9 N load.

Figure 5 shows the worn image of the CrNi3MoVA steel and CoCrFeNiW coating under a macroscopic scale. As shown in Fig. 5, with the increase of loads, the width of grinding marks becomes bigger on the surface of the CrNi3MoVA steel. Comparatively, it is hard to observe the grinding marks under a macroscopic scale on the surface of the CoCrFeNiW coating. Therefore, the CoCrFeNiW coating notably increases

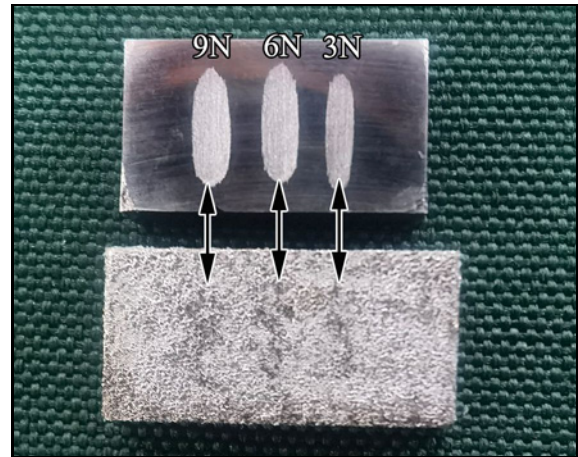


Fig. 5. Worn image of CrNi3MoVA steel and CoCrFeNiW coating under macroscopic scale.

the wear resistance of the CrNi3MoVA steel.

Although the samples of the worn CoCrFeNiW coating were placed into a container of alcohol and acetone mixture and cleaned by ultrasonic wave for 30 minutes, no weight loss was measured by an electronic balance (Sartorius BP211D) with a sensitivity of  $10^{-5}$  g. Weight gain was measured for the worn CoCrFeNiW coating, indicating that some wear debris adhered firmly to the worn CoCrFeNiW coating surface. The reasons for the weight gain in the CoCrFeNiW coating may be from two reasons: for one reason, as shown in Fig. 1b, there are many micro-holes on the surface of the CoCrFeNiW coating, the fine wear debris can be sintered in the micro-holes under the pressure of the rubbing load, and cannot be cleaned off by ultrasonic wave; for the other reason, the oxidation takes place on the surface of the CoCrFeNiW coating, for the CoCrFeNiW coating is easy to oxidize under the heat effect produced by the rubbing load.

Figure 6 shows the worn morphologies of the CrNi3MoVA steel at different magnifications. As shown in Fig. 6a, a severe plastic deformation occurs, and there are furrows due to the material piling up on the surface of the CrNi3MoVA steel. Region F in Fig. 6a is magnified to obtain Fig. 6b, in which a shear lip is observed on the worn surface of the CrNi3MoVA steel. The worn feature suggests that the main wear mechanism of the CrNi3MoVA steel belongs to severe adhesive wear.

Figure 7 shows the worn morphologies of the CoCrFeNiW coating at different magnifications. As shown in Fig. 7a, there is much wear debris (marked with arrows) in the dents on the uneven surface of the worn CoCrFeNiW coating. Figure 7b shows the magnified region G in Fig. 7a. As shown in Fig. 7b, no obvious scratches are observed on the protruding parts of the CoCrFeNiW coating surface. Furthermore, the

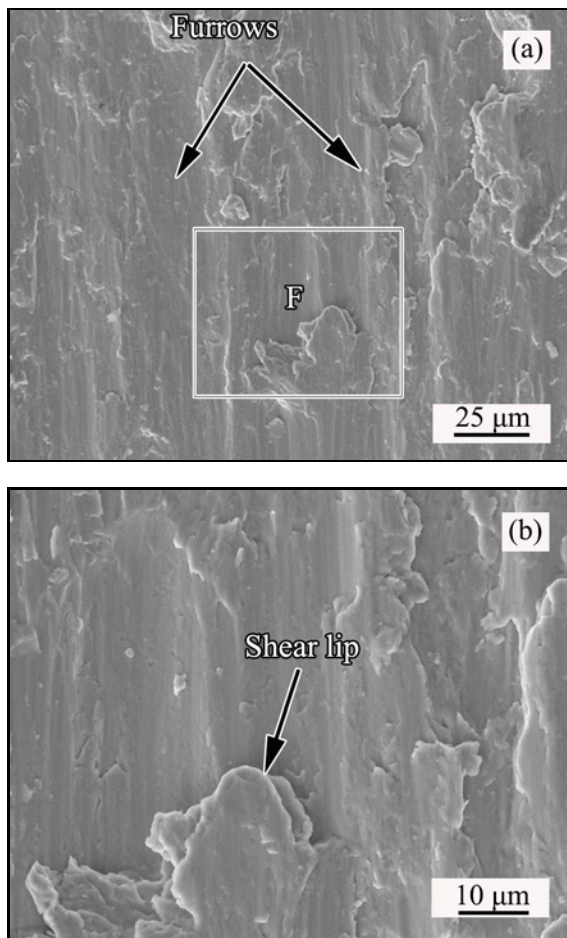


Fig. 6. Worn morphologies of CrNi3MoVA steel at low (a) and high (b) magnifications.

EDS results of region J show that the worn surface of the CoCrFeNiW coating contains the extra O element in contrast to the as-deposited CoCrFeNiW coating, which indicates that oxidation took place on the CoCrFeNiW coating surface during rubbing. Figure 7c shows the magnified region H in Fig. 7a. As shown in Fig. 7c, the size of the majority wear debris in the dents is below 10 microns, and the EDS results of the wear debris (region I) show that the wear debris mainly contains the elements of Fe, Ni, and Cr, suggesting that the wear debris is the worn product of the 304 stainless steel ball. Kato [16] and Hiratsuka and Muramoto [17] proposed that small wear particles generated in the wear stage were easily oxidized under the heat effect produced from rubbing, and they attached to the worn surface and formed an oxide film, which can induce mild wear. Their view is consistent with the results of this study. Furthermore, the special characteristic of an ESD coating surface with micro-holes is that it can store small wear particles, further improving the tribological properties of the CoCrFeNiW coating. From the above analysis, it can be concluded that the wear mechanism of the CoCrFeNiW coating is

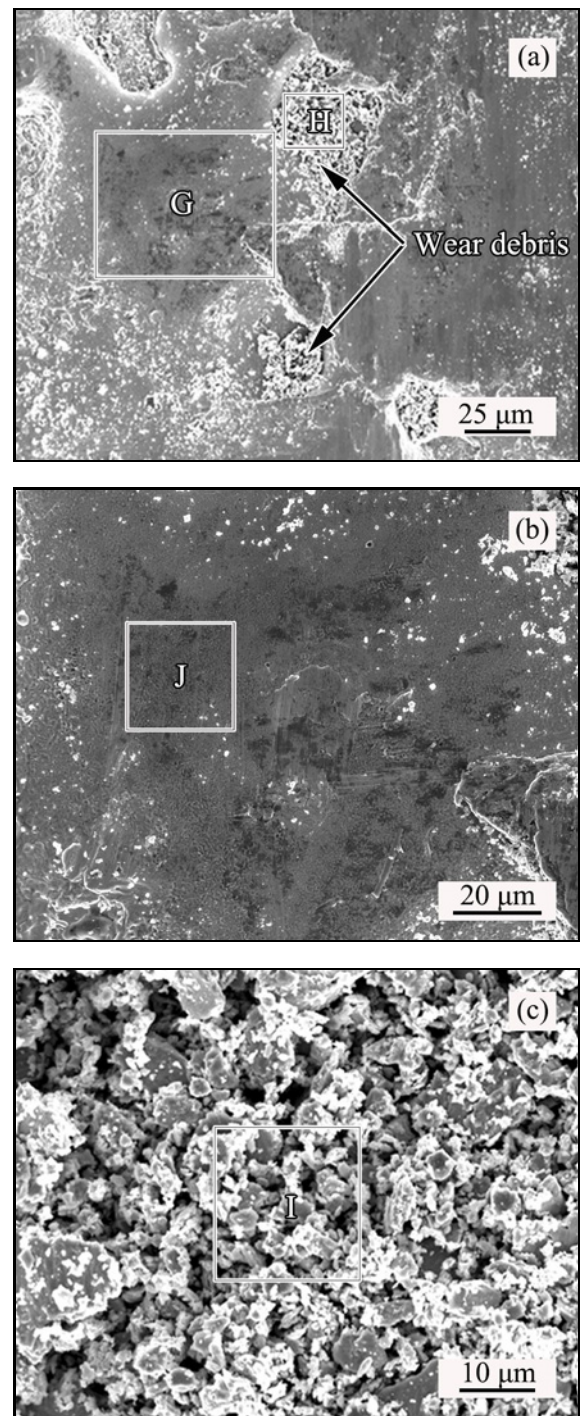


Fig. 7. Worn morphologies of CoCrFeNiW coating at low (a) and high (b), (c) magnifications.

slightly adhesive wear accompanying oxidation wear.

## 4. Discussion

### 4.1. Forming process of CoCrFeNiW coating

Figure 8 shows the preparation of the CoCrFeNiW

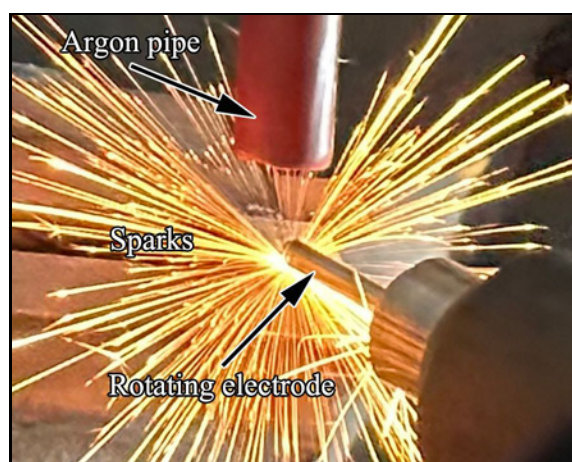


Fig. 8. Process of CoCrFeNiW HEA coating in argon.

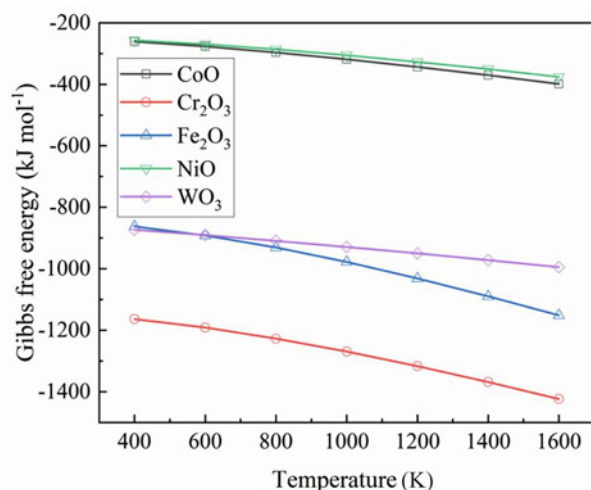


Fig. 9. Gibbs free energy change of oxides of Co, Cr, Fe, Ni, and W at various temperatures.

coating by ESD in argon. In this process, the CoCrFeNiW electrode and the CrNi3MoVA steel substrate come into contact at a small region in the form of a short circuit, and then the capacitor energy is instantaneously released. A plasma arc with a maximum temperature of 5000–25000 K is generated to produce a droplet formation at the end of the electrode [14, 18], and then it accelerates the droplet towards the substrate surface at high speed to form a splashing feature. At the same time, as the plasma temperature is high enough, the contacted substrate also melts with the electrode, and a small melting pool with electrode and substrate materials is formed. With the moving back and forth of the electrode, many melting pools connect to form the first deposition layer, and then the electrode moves on the previously formed layer to overlap, and the CoCrFeNiW coating is finally formed.

In this work, the composition of the CoCrFeNiW

coating is different from that of the electrode, for the coating cannot be kept growing thick due to metallurgy theory, so the content of Fe is more than that of the other four elements in the CoCrFeNiW coating. Due to the manual operation and uneven charge, the CoCrFeNiW coating surface appears to have an uneven morphology, which is a typical disadvantage for ESD technology.

Despite the argon protection, oxidation occurred on the CoCrFeNiW HEA coating surface, indicating that some oxygen is mixed in the ESD process. Figure 9 shows the Gibbs free energy change of Co, Cr, Fe, Ni, and W oxides at various temperatures [19]. As shown in Fig. 9, Cr<sub>2</sub>O<sub>3</sub> has the most negative Gibbs energy among the five formed oxides of the CoCrFeNiW coating so that it will be formed in the CoCrFeNiW coating (Fig. 2). Guo C. A. et al. [7] prepared AlCoCrFeNi coatings on CrNi3MoVA steel in argon by ESD technology and also found the Al<sub>2</sub>O<sub>3</sub> in the AlCoCrFeNi coating for Al<sub>2</sub>O<sub>3</sub> has the most negative Gibbs energy among the five formed oxides of the AlCoCrFeNi coating, which agrees with the result of this study.

#### 4.2. Wear resistance of CoCrFeNiW coating

It is well known that the cooling velocity of the ESD coating can reach  $10^5$ – $10^6$  K s<sup>-1</sup> [14, 18]. With such a rapid cooling speed, the crystal nuclei grow up with difficulty; thereby, the ESD coating always consists of micro-scale and even nano-scale structures [7, 14, 18], which favors the hardness increase of the coating. Besides the high hardness of the CoCrFeNiW coating, the values of  $H/E$  and  $H^3/E^2$  closely relate to the wear resistance of the materials. The value of  $H/E$  determines the elasticity limit of the rubbing contact surface, and a high  $H/E$  value reduces the quantity of the elasticity limit on the rubbing contact surface, which increases the wear resistance for antifriction; the value of  $H^3/E^2$  shows the capability to resist plastic deformation under the action of contact load [20, 21]. By calculating from Table 5, the  $H/E$  and  $H^3/E^2$  values of the CoCrFeNiW coating increase by about 1.4 and 10.3 times that of the CrNi3MoVA steel, respectively, which suggests that the CoCrFeNiW coating has better wear resistance than the CrNi3MoVA steel.

Apart from the excellent nanoindentation results, there are also two other reasons for the improved tribological properties of the CoCrFeNiW coating. On one hand, the compact Cr<sub>2</sub>O<sub>3</sub> oxide scale formed on the coating benefits the wear resistance. Like other ESD coatings [7, 14, 18], the microstructure of the CoCrFeNiW coating belongs to microcrystalline with columnar crystals, which favors the selective oxidation of Cr. On the other hand, the wear debris with a size of ten microns in the dents of the CoCrFeNiW HEA coating reduces the rubbing contact area of the

CoCrFeNiW coating, which can also increase the wear resistance of the coating.

## 5. Conclusions

The as-deposited CoCrFeNiW coating with an uneven surface has a chemical composition different from that of the sintered CoCrFeNiW electrode, which is composed of FCC and Cr<sub>2</sub>O<sub>3</sub>. Compared with the CrNi<sub>3</sub>MoVA steel, the hardness of the CoCrFeNiW coating increases about 1.1 times and the elasticity modulus reduces by 11.6%. The friction coefficients of the CoCrFeNiW coating (0.5) are much smaller than those of the CrNi<sub>3</sub>MoVA (0.7) steel at 6 and 9 N load. The CoCrFeNiW coating remarkably increases the wear resistance of the CrNi<sub>3</sub>MoVA steel at 3, 6, and 9 N load due to the excellent nanoindentation results, the compact Cr<sub>2</sub>O<sub>3</sub> oxide scale formed on the coating and the wear debris with a size of ten microns in the dents of the CoCrFeNiW coating. The mechanism of the CoCrFeNiW coating can be characterized as slight adhesive wear accompanied by oxidation wear, whilst that of the CrNi<sub>3</sub>MoVA steel belongs to severe adhesive wear. Compared with the conventional ESD coatings of hard alloys, such as WC-Co, or WC-TiC-Co, etc., the ESD CoCrFeNiW coating can form a compact Cr<sub>2</sub>O<sub>3</sub> oxide scale during rubbing, and it also has a strong bonding due to the better interinfiltration of the CoCrFeNiW electrode and the steel substrate, both of which can enhance the wear resistance of the coating.

## Acknowledgements

The authors are grateful for the financial support of the Research Project of Application Foundation of Liaoning Province of China (No. 2022JH2/101300006), the Research Project of Education Department of Liaoning Province of China (LJKMZ20220604 and 1030040000675), the Foundation of National Key Laboratory for Remanufacturing, the Key Laboratory of Weapon Science & Technology Research (LJ232410144071), and the Light-Selection Talents and Team Plan of Shenyang Ligong University (SY-LUGXTD5).

## References

- [1] J. W. Yeh, S. K. Chen, S. J. Lin, J. Y. Gan, T. S. Chin, T. T. Shun, C. H. Tsau, S. Y. Chang, Nanostructured high entropy alloys with multiple principal elements: Novel alloy design concepts and outcomes, *Advanced Engineering Materials* 6 (2004) 299–303. <https://doi.org/10.1002/adem.200300567>
- [2] B. Cantor, I. Chang, P. Knight, A. J. B. Vincent, Microstructural development in equiatomic multicomponent alloys, *Materials Science and Engineering A* 375–377 (2004) 213–218. <https://doi.org/10.1016/j.msea.2003.10.257>
- [3] H. Liu, Q. Gao, J. Dai, P. Chen, W. Gao, J. Hao, H. Yang, Microstructure and high-temperature wear behavior of CoCrFeNiW<sub>x</sub> high-entropy alloy coatings fabricated by laser cladding, *Tribology International* 172 (2022) 107574. <https://doi.org/10.1016/j.triboint.2022.107574>
- [4] X. Wang, B. Huang, T. Li, Y. Wu, X. Hong, J. Zheng, Y. Zhu, Effect of heat treatment on microstructure and properties of CrMnFeCoNiMo high entropy alloy coating, *Journal of Materials Research and Technology* 29 (2024) 311–322. <https://doi.org/10.1016/j.jmrt.2024.01.123>
- [5] A. A. Burkov, P. G. Chigrin, M. I. Dvornik, Electrospark CuTi coatings on titanium alloy Ti6Al4V: Corrosion and wear properties, *Surface and Coatings Technology* 469 (2023) 129796. <https://doi.org/10.1016/j.surfcoat.2023.129796>
- [6] M. A. Fomina, V. A. Koshuro, A. A. Fomin, Superhard Ti-Ta-O coatings produced on titanium with electrospark deposited tantalum-containing layers using induction heat treatment, *International Journal of Refractory Metals and Hard Materials* 115 (2023) 106314. <https://doi.org/10.1016/j.jirmhm.2023.106314>
- [7] H. L. Yang, X. M. Chen, L. Chen, Z. J. Wang, G. C. Hou, C. A. Guo, J. Zhang, Influence of temperature on tribological behavior of AlCoCrFeNi coatings prepared by electrospark deposition, *Digest Journal of Nanomaterials and Biostructures* 18 (2023) 145–156. <https://doi.org/10.15251/DJNB.2023.181.145>
- [8] F. Abdi, H. Aghajani, A. T. Tabrizi, L. Nasimi, F. F. Shokouhi, Study on the effect of the crack closing of AlCoCrFeMnNi high entropy alloy electro-spark deposited coating by plasma nitriding on the corrosion resistance, *Journal of Alloys and Compounds* 966 (2023) 171629. <https://doi.org/10.1016/j.jallcom.2023.171629>
- [9] F. Abdi, H. Aghajani, S. K. Asl, Evaluation of the corrosion resistance of AlCoCrFeMnNi high entropy alloy hard coating applied by electro spark deposition, *Surface & Coatings Technology* 454 (2023) 129156. <https://doi.org/10.1016/j.surfcoat.2022.129156>
- [10] A. A. Burkov, P. G. Chigrin, M. A. Kulik, Effect of TaC content on microstructure and wear behavior of PRMMC Fe-TaC coating manufactured by electrospark deposition on AISI304 stainless steel, *Surface & Coatings Technology* 494 P2 (2024) 131446. <https://doi.org/10.1016/j.surfcoat.2024.131446>
- [11] F. Zhou, B. N. Xing, C. A. Guo, C. X. Du, L. Z. Xu, Z. H. Du, G. F. Gao, Investigation on the influence of electrospark deposited 718 alloy coating on the penetration performance of 93 W rod, *International Journal of Refractory Metals and Hard Materials* 125 (2024) 106882. <https://doi.org/10.1016/j.jirmhm.2024.106882>
- [12] K. Korkmaz, Investigation and characterization of electrospark deposited chromium carbide-based coating on the steel, *Surface & Coatings Technology* 272 (2015) 1–7. <http://dx.doi.org/10.1016/j.surfcoat.2015.04.033>
- [13] O. M. Myslyvchenko, O. P. Gaponova, V. B. Tarelnyk, M. O. Krapivka, The structure formation and hardness of high-entropy alloy coatings obtained by electrospark deposition, *Powder Metallurgy and Metal*

- Ceramics 59 (2020) 201–208.  
<http://doi.org/10.1007/s11106-020-00152-7>
- [14] C. A. Guo, T. Liang, F. Lu, Z. Liang, S. Zhao, J. Zhang, Isothermal oxidation behavior of electrospark deposited NiCrAlY coatings on a Ni-based single-crystal superalloy, *Materials and Technology* 53 (2019) 389–394. <https://doi.org/10.17222/mit.2018.210>
- [15] Y. J. Xie, M. C. Wang, Isothermal oxidation behavior of electrospark deposited MCrAlX-type coatings on a Ni-based superalloy, *Journal of Alloys and Compounds* 480 (2009) 454–461.  
<https://doi.org/10.1016/j.jallcom.2009.01.100>
- [16] H. Kato, Effects of supply of fine oxide particles onto rubbing steel surfaces on severe-mild wear transition and oxide film formation, *Tribology International* 41 (2008) 735–742.  
<https://doi.org/10.1016/j.triboint.2008.01.001>
- [17] K. Hiratsuka, K. Muramoto, Role of wear particles in severe-mild wear transition, *Wear* 259 (2005) 467–476.  
<https://doi.org/10.1016/j.wear.2005.02.102>
- [18] R. Wang, Q. Liu, M. Wang, X. D. Lu, C. A. Guo, J. Zhang, High-temperature oxidation behavior of an N5 Nanocrystalline coating deposited with ESD on a Ni-based single-crystal superalloy, *Materials and Technology* 55 (2021) 733–740.  
<https://doi.org/10.17222/mit.2021.171>
- [19] Y. J. Liang, Y. C. Che, *Handbook of Inorganic Compound of Thermodynamic Data*, 1st ed., Northeastern University, Shenyang 1993.
- [20] A. Leyland, A. Matthews, On the significance of the  $H/E$  ratio in wear control: A nanocomposite coating approach to optimised tribological behaviour, *Wear* 246 (2000) 1–11.  
[https://doi.org/10.1016/S0043-1648\(00\)00488-9](https://doi.org/10.1016/S0043-1648(00)00488-9)
- [21] L. Ipaz, J. C. Caicedo, J. Esteve, F. J. Espinoza-Beltran, G. Zambrano, Improvement of mechanical and tribological properties in steel surfaces by using titanium-aluminum/titanium-aluminum nitride multilayered system, *Applied Surface Science* 258 (2012) 3805–3814.  
<https://doi.org/10.1016/j.apsusc.2011.12.033>